Properties of dense partially random graphs

Sebastián Risau-Gusman*
Instituto de Física, Universidade Federal do Rio Grande do Sul, CP 15051, 91501-970 Porto Alegre, RS, Brazil
(Received 6 July 2004; published 23 November 2004)

We study the properties of random graphs where for each vertex a *neighborhood* has been previously defined. The probability of an edge joining two vertices depends on whether the vertices are neighbors or not, as happens in small-world graphs (SWG's). But we consider the case where the average degree of each node is of order of the size of the graph (unlike SWG's, which are sparse). This allows us to calculate the mean distance and clustering, which are qualitatively similar (although not in such a dramatic scale range) to the case of SWG's. We also obtain analytically the distribution of eigenvalues of the corresponding adjacency matrices. This distribution is discrete for large eigenvalues and continuous for small eigenvalues. The continuous part of the distribution follows a semicircle law, whose width is proportional to the "disorder" of the graph, whereas the discrete part is simply a rescaling of the spectrum of the substrate. We apply our results to the calculation of the mixing rate and the synchronizability threshold.

DOI: 10.1103/PhysRevE.70.056127 PACS number(s): 89.75.Hc, 02.50.−r, 05.45.Xt

I. INTRODUCTION

Many natural and artificial systems are composed of a large number of identical agents that interact. Examples of this kind of system are numerous and widespread: collaborators in physics, neural networks, computer programs (considered as a system of interacting subroutines), the World Wide Web, movie actors, etc.

The interactions, however, need not be identical and can vary in strength and range. A simplified analysis of such a system can take into account only the pattern of interactions, abstracting everything else. What is left is usually called a *network* and is mathematically represented by a *graph* (along this article both terms will be used interchangeably.)

A graph is composed of *vertices* (associated to the agents) connected by *edges*. Agents only interact with other agents if there is an edge joining the corresponding vertices, and the strength of the interaction is given by the *weight* of the edge. The interactions between graph theory and physical science, particularly physics, has been very fruitful [1].

In 1959 Erdös and Renyi [2] started a whole new branch of graph theory by creating (and extensively studying) the concept of *random graphs*. These are graphs where each edge has a defined probability of being present, and this probability is independent of all other edges. They seem particularly well suited for the study of systems for which there is little information about the range of the interactions. In these cases it seems natural to assign independent and equal probabilities to the different connections.

The average distance of a graph is defined as the average of the length (i.e., the number of vertices) of the smallest path joining two edges. The clustering coefficient gives the average number of connections present between neighbors of a vertex, divided by the number of possible connections within the neighborhood of the vertex. In their groundbreaking article of 1998, Watts and Strogatz (WS) [3] showed that most real networks display a very short average distance combined with large values of the clustering coefficient. But random graphs do not fulfill these requirements because, even though the average distance is short, the clustering coefficient turns out to be rather small. Thus they proposed a new graph model, the small world graph (SWG). To build a SWG one starts with a regular and *sparse* substrate graph (with large clustering but also with large average distance) and then rewires some edges with a probability p, thus creating shortcuts. It was shown that a small number of shortcuts is enough to significantly lower the average distance while leaving the clustering coefficient almost unchanged.

Since their proposal, the properties of SWG's have been intensively studied with numerical as well as analytical methods. Even though some numerical analyses have been performed [4], one of the properties that still resists analytical treatment is the spectrum of the adjacency matrix of SWG's.

The constraint of sparsity is justified by the fact that many networks in nature display this characteristic. But one can also find systems where the pattern of connections of every node spans a significant portion of the whole graph (i.e., the degree of the nodes is of the same order as the size of the network). Some examples of this are the network of train routes in India [5], the full reaction graphs of the metabolic network of *E. coli* [6,7], and the network of the interacting units of the computer program MOZILLA [8].

In this article we study the properties of graphs for which the sparsity constraint has been dropped. This allows us to calculate analytically the average distance and the clustering coefficient, as well as the whole eigenvalue distribution of the corresponding adjacency matrices. The spectra of these matrices can be considered as limiting cases of the ones of sparse SWN's.

The values of the different properties calculated in this article are only *averages* over a certain family of graphs (defined in the next section). Nevertheless, simulations support the idea that the properties of almost every graph of this family should tend, in probability, to the average values found.

*Electronic mail: srisau@if.ufrgs.br

In Sec. II we define the model and relate it to the Watts-Strogatz prescription. In Sec. III we calculate the average distance and the clustering coefficient. In Sec. IV we obtain the spectrum of the corresponding adjacency matrices and compare it to the spectrum of sparse graphs. A couple of applications of the results obtained are presented in Sec. V. In Sec. VI some conclusions are drawn.

II. MODEL

A graph is a pair of sets (V,E), where V has N elements (or vertices) and $E \subseteq V^2$ has M elements (or edges). Two vertices v_1 and v_2 are connected if $(v_1,v_2) \in E$.

WS [3] proposed a graph model capable of interpolating between order and randomness. The graphs in this model are built by taking a *substrate*, which is a graph displaying some regularity, and randomly *rewiring* some of its edges, by keeping fixed one end of some edges and redirecting the other end to a different vertex at random, but following some rule. Let us consider, for example, the unidimensional case, where each vertex in a ring is connected to $k/2$ vertices to the left and $k/2$ vertices to the right. The process begins by traveling clockwise on the ring and, for each vertex rewiring, with probability p, the connection that joins it with its first neighbor to the right. Once the circle is completed, a new round is made where now the connection rewired is the one to the second neighbor to the right. The process ends after $k/2$ rounds (because $k/2$ is the number of neighbors to the right). A similar process can be implemented for a higher-dimensional substrate. The graph obtained is called a SWG.

In our model of dense partially random graphs (DPRG's), we only consider hypercubic lattices as substrates, with the hope that for other substrates things will not be very different, as is the case for sparse SWG [9]. In these lattices $V \subset \mathbb{R}^d$ and each dimension has a different connectivity parameter k_i, which means that each node is connected to a hypercube of $k=\Pi_{i=1}^{d} k^i - 1$ nodes. This defines a k-neighborhood for each vertex. As opposed to the usual constraint of considering sparse networks, here we are concerned only with *dense* graphs—i.e., graphs where each vertex is connected to $k=O(N)$ other vertices. Notice that, to have the same number of neighbors for all nodes, we are considering periodical boundary conditions for the lattices. Thus, the one-dimensional lattice is formed by points on a ring, the two-dimensional lattice by points on a torus, etc.

We randomize the graph in the following way: each edge in every k-neighborhood is deleted with a probability $1-p_1$ and vertices that do not belong to the same k-neighborhood are joined with probability p_2. This is equivalent to saying that, on an empty graph, each vertex is joined by a *short* link with probability p_1 to every vertex in its k-neighborhood and with probability p_2 to those outside it, by a *long* link or *shortcut*. A graph generated with this prescription is called $G_{p_1 p_2}(\gamma)$, with $\gamma=k/N$. The family of all such graphs, for p_1, p_2, and γ fixed, is called $\mathcal{G}_{p_1 p_2}(\gamma)$. With $p_1=1$ and $p_2=0$ one obtains the ordered substrate, whereas for $p_1=p_2=k/N$ one obtains a random graph [10].

Notice that each vertex has a different number of connections, whose average number is $kp_1+(N-1-k)p_2 \sim N[\gamma p_1 + (1-\gamma)p_2]$. But in the limit treated in this article, of large values of N, the deviations from this average value are exponentially small. To interpolate with only one parameter between a fully ordered and a fully random graph, we fix this average value by requiring that $\gamma p_1+(1-\gamma)p_2=\gamma$ (along the paper, though, results will be displayed for general p_1 and p_2, unless otherwise stated). Notice that in this case the average number of connections of each vertex is k. Choosing p_1 as the preferred parameter, a graph satisfying the relationship shown above is called $G_{p_1}(\gamma)$ and the family of graphs with p_1 and γ fixed is called $\mathcal{G}_{p_1}(\gamma)$. As mentioned, for $p_1=\gamma$ the family $\mathcal{G}_{p_1}$ [10] of completely random graphs is obtained.

In our model the number of shortcuts is $p_2 N$, for large N. To be able to compare the graphs in $\mathcal{G}_{p_1}(\gamma)$ with SWG's, it is necessary to know the number of shortcuts of the graphs generated with the WS prescription. In the sparse case, it is known that this number is $\sim pkN/2$. This comes from the fact that the sparsity of the network ensures that when a link is selected, the probability that it will be rewired to a vertex inside the same k-neighborhood is $\sim 1/N$. But if the network is dense, this probability becomes nonvanishing. The following procedure provides a good approximation to the number of shortcuts.

Instead of disconnect and rewire the links sequentially in each round, let us assume that in each round pN short edges are deleted *at once* and then pN *random* edges are added, which can be short or long. The process begins with only the $S=kN/2$ short edges present in the graph. We call S_t the number of short edges after round t and L_t the number of long edges. Notice that after deleting pN short edges, the probability that one of the random edges added is short is the quotient between the number of available short edges and the number of total available edges: $(pN+S-S_t)/(L+S-S_t-L_t+pN)=(pN+S-S_t)/(L+pN)$, where $L=N(N-1)/2-S$. We are using the fact that the number of edges is conserved $(S_t+L_t=S)$. Using this, the evolution equations for large enough N can be obtained:

$$S_{t+1} = S_t - pN + pN\frac{pN+S-S_t}{L+pN}, \tag{1}$$

$$L_{t+1} = S - S_{t+1}. \tag{2}$$

The second summand in Eq. (1) corresponds to the edges deleted and the third to the fraction of edges added that are short. This formula can be iterated to obtain

$$S_{t+1} = S - L + L\left(\frac{L}{L+pN}\right)^{t+1}. \tag{3}$$

After $t=k/2$ rounds and in the limit of large k and N such that $\gamma=k/N$, we obtain

$$p_1 = S_k/S \sim 1 - \frac{1-\gamma}{\gamma}\left[1-\exp\left(-\frac{\gamma p}{1-\gamma}\right)\right], \tag{4}$$

$$p_2 = L_k/L \sim 1 - \exp\left(-\frac{\gamma p}{1-\gamma}\right). \tag{5}$$

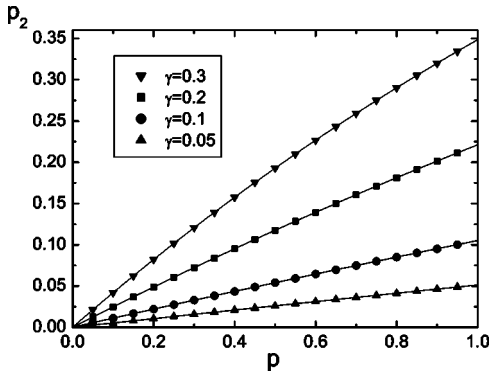

FIG. 1. Fraction of shortcuts as a function of the rewiring probability p. The symbols are averages taken on 30 matrices with $N=6001$. The lines are the theoretical predictions. Error bars are smaller than the symbols.

Figure 1 shows that the agreement with the real number of shortcuts for dense SWG's is very good. Thus, in what follows, to translate the results of our model to dense small-world graphs, it suffices to take p_2 and invert Eq. (5) to obtain the corresponding p. Notice that for values of p close to 1 there is some "overshooting," as the resulting SWG's have more shortcuts than the corresponding random graphs (i.e., $p_2 > \gamma$).

III. TOPOLOGICAL PROPERTIES

A. Average distance

For random graphs with a number $O(N^2)$ of edges, it is known that the diameter (i.e., the largest distance between any two nodes) is equal to 2, for large values of N. This means that from any vertex only 1 or 2 steps are needed to reach any other vertex. This in turn implies that the average distance in such a graph tends to $2-p$. For a general graph it is known [11] that $2-p$, with $p=2M/N(N+1)$, is a lower bound to the average distance. It is interesting to notice that this bound is achieved by some graphs (stars, for example). Random graphs, on the other hand, only achieve it in the limit of infinite N. In our model this implies that the average distance satisfies $\bar{d} \geqslant 2-p_1\gamma-p_2(1-\gamma)$.

The graphs in $\mathcal{G}_{p_1p_2}(\gamma)$ can be generated as the union of two random graphs. One of them is simply a completely random graph with edge probability p_2, called G_{p_2}. For the other, the probability that an edge is present is 0 if it is a long edge and $p=(p_1-p_2)/(1-p_2)$ if it is a short edge. This union results in a graph equivalent to the one obtained by adding a number N_a of edges to G_{p_2}, such that $\bar{N}_a=(1-p_2)p\gamma$. Now every one of these additional edges has the effect of decreasing the average distance of the graph by at least M^{-1}. Thus, averaging over all graphs in $\mathcal{G}_{p_1p_2}(\gamma)$, the mean average distance must satisfy $\bar{d} \leqslant 2-p_2-\gamma p(1-p_2)=2-p_1\gamma-p_2(1-\gamma)$. This, together with the upper bound, implies that, in mean, $\bar{d}=2-p_1\gamma-p_2(1-\gamma)$ for large N. The fact that this value is a lower bound for general graphs ensures that, for large values of N, almost every graph has an average distance equal to the mean.

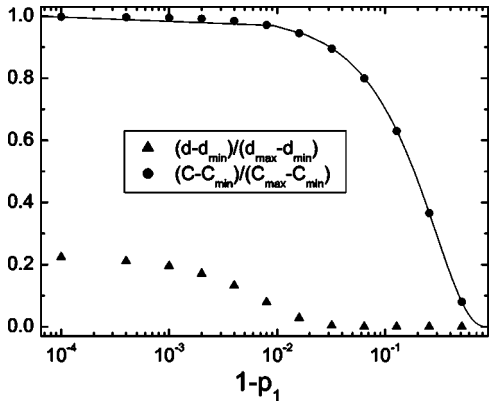

FIG. 2. Average random distance and clustering coefficient for graphs $G_{p_1}(\gamma)$, scaled by their maximum and minimum values. The symbols are averages taken on 30 matrices with $N=6001$ and $\gamma=0.1$. The line is the theoretical prediction for the average distance. Error bars are smaller than the symbols.

Notice that for graphs in $\mathcal{G}_{p_1}(\gamma)$, in the infinite-$N$ limit, the average distance for $p_1<1$ is only a function of γ: $\bar{d}=2-\gamma$. For $p_1=1$ and $p_2=0$, the graph is circulant, and it is not difficult to see that the average length is $(1+\gamma)/2\gamma$ [9]. In Fig. 2 it can be seen that for finite but large values of N, the average distance falls very rapidly with the number of shortcuts.

B. Clustering coefficient

The average distance can be thought of as a *global* property of a graph: it gives an idea of how far apart is any vertex from any other. The *clustering coefficient* provides a different kind of information: it is a measure of how locally connected is the graph. It is obtained by calculating, for every vertex of the graph, the number of links joining points of its neighborhood divided by the total number of possible links in the neighborhood and taking its average over all vertices. This gives the probability that two neighbors of a vertex are connected to each other. It can be shown [12] that this is equivalent to calculating the total number of triangles in the graph, divided by the total number of paths of length 2 (hereafter called 2-paths).

Instead of calculating this number for every graph and then averaging over the ensemble, we calculate an "annealed" version of it [13]: we take the average of the number of triangles and divide it by the average number of 2-paths. For large values of N the agreement with the numerical values turns out to be very good (see Fig. 2).

To calculate the number of 2-paths, one has to find the number of 2-paths for every matrix, weigh it with the probability of that matrix, and then sum over all possible graphs. An equivalent way of doing this is to sum over all possible paths, with a weight given by $p_1^i p_2^{2-i}$, where i is the number of long links in the path.

In the limit of infinite N all vertices are equivalent and it is enough to consider all the paths beginning from a fixed vertex and then multiply by N. To count these paths, one needs to know the size of the intersection of the

k-neighborhoods of two points. If $\gamma < 2^{-d}$, this intersection is a connected region and the calculation of its size is very simple. We analyze only this case, because one is usually interested in low dimensions. For bigger values of γ the calculations are straightforward but much more cumbersome.

Assuming the fixed vertex located at the origin and its other end at a position $\vec{x} \in \mathbb{Z}^d$, the size of the intersection of the two k-neighborhoods is

$$I(\vec{x}) = \begin{cases} \prod_{i=1}^{d} I_i(\vec{x}), & \vec{x} \in \Gamma_k(0), \\ \prod_{i=1}^{d} I_i(\vec{x}) - 2, & \vec{x} \in \Gamma_{2k}(0) - \Gamma_k(0), \\ 0, & \vec{x} \in \Gamma_{2k}(0), \end{cases} \tag{6}$$

where $\Gamma_k(0)$ is the set of nodes that form the k-neighborhood of the origin and

$$I_i(\vec{x}) = 2k_i - |x_i| + 1. \tag{7}$$

Using this, we obtain that the total number of 2-paths is, to first order in N,

$$N_p = \sum_{\vec{x} \in G} \Pi(\vec{x}) \{ p_1^2 I(\vec{x}) + 2p_1 p_2 [|\Gamma_k| - I(\vec{x})] + p_2^2 [N - 2|\Gamma_k| + I(\vec{x})] \}, \tag{8}$$

with $\Pi(\vec{x}) = 1$. The first term in the curly brackets counts the number of paths with two short edges, the second counts the paths with one short and one long edge, and the third counts those paths with two long edges. To calculate the number of triangles one proceeds in exactly the same way, but it must now be assumed that the endpoints of the paths are connected by an edge. Thus, the number of triangles is given by Eq. (8) using $\Pi(\vec{x}) = 1 - p_1$ for $\vec{x} \in \Gamma_k(0)$ and $\Pi(\vec{x}) = 1 - p_2$ for $\vec{x} \in V - \Gamma_k(0)$. After some algebra the clustering coefficient obtained is

$$C = \frac{\gamma_d^2 (p_1 - p_2)^3 [(3/4)^d - \gamma_d] + [(p_1 - p_2)\gamma_d + p_2]^3}{[(p_1 - p_2)\gamma_d + p_2]^2}, \tag{9}$$

with

$$\gamma_d = \prod_{i=1}^{d} \gamma_i. \tag{10}$$

In the case of a graph $G_{p_1}(\gamma)$ the clustering coefficient simplifies to

$$C = (p_1 - p_2)^3 [(3/4)^d - \gamma_d] + \gamma_d. \tag{11}$$

A comparison with data obtained from graphs with 6001 vertices can be seen in Fig. 2. Theory and data only differ where $1 - p_1 \simeq (\gamma N)^{-1}$, where our approximations do not hold.

IV. SPECTRUM OF THE GRAPH

For a graph with no loops and with no multiple edges, as those treated in this article, the adjacency matrix A is a 0-1 matrix where $A_{ij} = 1$ if there is an edge connecting vertices i and j, and 0 otherwise. Diagonal elements are set to 0. The eigenvalues of A provide a lot of information about the structure of the graph (see Ref. [14]). For example, if the graph is regular and its eigenvalue distribution is symmetric, then the graph is bipartite. Eigenvalues also provide useful bounds to quantities as different as the diameter of a graph [15] and the mixing rate [16] of random walks. In the following section we summarize some results for the spectrum of circulant graphs which will be useful in our determination of the spectrum of DPRG's.

A. Circulant graphs

The family of circulant graphs is one of the few for which all the eigenvalues and eigenvectors can be calculated analytically [17]. The adjacency matrix of such a graph is a *circulant* matrix, where row i is simply the first row shifted i places to the right. In our case, the adjacency matrices of the graphs with $p_1 = 1$ and $p_2 = 0$ are circulant. They are symmetric matrices with null diagonal elements, satisfying, for $d = 1$ and $j > i$, $A_{ij} = 1$ for $j - i \leqslant k/2$ and 0 otherwise.

The eigenvectors of these matrices are N vectors $\vec{v}_j = (1, \rho_j, \rho_j^2, \ldots, \rho_j^{N-1})$ for $0 \leqslant j \leqslant N-1$, with $\rho_j = \exp(2\pi j/N)$. Interestingly, all circulant matrices have the same eigenvectors. This is not the case for the eigenvalues, which satisfy $\lambda_j^c = \Sigma_{i=1}^{N} A_{ji} \rho_j^{i-1}$. In our case, this gives

$$\lambda_j^c = \rho_j^{-(k/2+1)} \sum_{i=1}^{N} e^{i\pi ki/N} = 2\cos\left(\frac{\pi j(k/2+1)}{N} \right) \frac{\sin(\pi jk/2N)}{\sin(\pi j/N)}. \tag{12}$$

Except for the first one, the Perron-Frobenius eigenvalue $\lambda_0^c = k$, all the other eigenvalues satisfy $\lambda_j^c = \lambda_{N-j}$ (we consider only odd values of N). Thus, there are $(N-1)/2$ eigenvalues with multiplicity equal to 2. For $j \ll N$ we have

$$\frac{\lambda_j^c}{N} = \frac{\sin(\pi j\gamma)}{\pi j} - 2\frac{\sin^2(\pi j\gamma/2)}{N} - \frac{\pi j \sin(\pi j\gamma)}{3N^2} + O\left(\frac{j^3}{N^4} \right). \tag{13}$$

For $j = O(N)$, it can be seen from Eq. (12) that $\lambda_j^c = O(1)$.

For $d > 1$ our substrates are reticles where the range of connection of each node depends on the spatial direction i, through a variable k_i. The adjacency matrices for these graphs are simply the Kronecker product (or tensor product) of the corresponding $N^{1/d} \times N^{1/d}$ matrices for each direction: $A = A(k_1) \otimes A(k_2) \otimes \ldots \otimes A(k_N)$. The resulting matrix is circulant and has the nice property that its eigenvalues are

$$\lambda_{j_1 j_2 \ldots j_d}^c = \prod_{i=1}^{d} \lambda_{j_i}^c \quad \text{for } 1 \leqslant j_i \leqslant N, \tag{14}$$

where the $\lambda_{j_i}^c$'s are given by Eq. (12).

B. Dense partially random graphs

The moments M_j of an $N \times N$ matrix A are defined by

$$M_j = N^{-1} \mathrm{Tr}(A^j) = N^{-1} \sum_{i=0}^{N} \lambda_i^j. \tag{15}$$

The jth power of an adjacency matrix gives information about all the possible paths of length j in the associated graph. More specifically, $(A^j)_{ik}$ is the number of j-paths that connect vertices i and k. Thus, the trace of the jth power of A is the total number of closed paths, called *cycles*, of length j.

If, for an ensemble of matrices, the calculation of the average number of cycles can be performed for every length, by using the averaged version of Eq. (15) it is possible to obtain the average distribution of eigenvalues. This is the route taken by Wigner [18] in his famous derivation of the semicircle law for random matrices. His work was afterwards extended [19] to prove that for large matrices the distribution of eigenvalues of *almost every* matrix of the ensemble tends to the semicircle. In Ref. [20] the same method was used to calculate the moments of random 0-1 matrices.

In both these works and in many others, all the cycles are characterized as sequences of vertices. For each sequence of length j the statistical weight is the same, as all the edges in the graph have the same probability of being present.

In our model this is different because short and long links have different probabilities. Therefore, in our case it is better to characterize each cycle as a succession of *distances*. We begin by analyzing the unidimensional case, and afterwards we indicate the modifications necessary to extend the results to higher dimensions.

On a ring, vertices can be consecutively labeled with numbers from 1 to N by going round the circle. When standing on a vertex, a walker can only make a step to the right or to the left. The distance between vertices i and j is defined as $d_{ij}=\min(|i-j|,N-|i-j|)$. Intuitively, it is the shortest number of consecutive vertices, including the end vertex, that a walker must traverse to go from i to j. To define a direction we say that if a walker, using an existing link, goes from vertex i to vertex j such that $(i-j) \bmod N \leqslant (N-1)/2$, then he has made a step to the *right*, covering a distance d_{ij}. Otherwise, we say that he has traveled to the left, covering a distance d_{ij}. Thus, a j-path can be defined by a succession of j distances. The total distance traveled is the sum of the signed distances.

If the path is a closed one—i.e., a cycle—the total signed distance must be equal to mN, because the cycle can contain m complete rounds of the circle. In a cycle traversing i long edges, called a ji-cycle, the number of complete rounds will be bounded by $m_{\max}=\lfloor (j-i)\gamma/2+i(N+1)/(2N) \rfloor$, where $\lfloor x \rfloor$ gives the largest integer smaller than or equal to x. P_{ji} is defined as the number of ji-cycles for a fixed position in the cycle of the i long links. Because the probabilities for each edge are independent, P_{ji} does not depend on the actual positions of the long links. As the probability of a ji-cycle is $p_1^{j-i}p_2^i$, the average over $\mathcal{G}_{p_1p_2}(\gamma)$ of the jth moment is

$$\overline{M_j}=\sum_{i=0}^{j}\binom{j}{i}p_1^{j-i}p_2^i\overline{P_{ji}}. \tag{16}$$

As explained in the Introduction, all the quantities calculated in this article are averages. Thus, hereafter we drop the overlines to avoid overloading the notation.

Let us call d_l the distance traveled in the lth step. To long links there correspond signed distances satisfying $k<|d_l| \leqslant N/2$. For short links, the corresponding distances satisfy $1 \leqslant |d_l| \leqslant k$. Thus, P_{ji} is the number of solutions $\vec{d} \in \mathbb{Z}^j$ of the problem

$$\sum_{l=1}^{j} d_l = mN \quad \text{for } |m| < m_{max},$$

$$1 \leqslant |d_l| \leqslant k/2 \quad \text{if } 1 \leqslant l \leqslant i,$$

$$k/2 < |d_l| \leqslant (N-1)/2 \quad \text{if } i < l \leqslant j. \tag{17}$$

Using the principle of inclusion and exclusion [21], P_{ji} can be written as

$$P_{ji}=\sum_{l=0}^{i}(-1)^{i-l}\binom{i}{l}\tilde{P}_{jl}, \tag{18}$$

where $\tilde{P}_{jl}$ is the number of solutions to the simpler problem

$$\sum_{l=1}^{j} d_l = mN \quad \text{for } |m| < m_{max},$$

$$1 \leqslant |d_l| \leqslant k/2 \quad \text{if } 1 \leqslant l \leqslant i,$$

$$1 < |d_l| \leqslant (N-1)/2 \quad \text{if } i < l \leqslant j. \tag{19}$$

$\tilde{P}_{ji}$ corresponds to the number of cycles where $j-i$ fixed steps use short links, whereas the other steps can use either long or short links. It is not difficult to see that $\tilde{P}_{ji}$ is of order N^{j-1} (as the path is closed, only $j-1$ steps may be freely chosen). Notice that d_l cannot be zero because loops are not allowed. But the presence of loops only adds to P_{ji} terms of order jN^{j-2}. As we are only interested in the dominating term, we include the loop terms, that allow for simpler calculations. Using this and rescaling the distances, the problem of Eq. (19) can be rewritten as the number of solutions of

$$\sum_{l=1}^{j} d_l = i(k/2+1)+(j-i)(N+1)/2+mN \quad \text{for } |m| < m_{max},$$

$$1 \leqslant d_l \leqslant k+1 \quad \text{if } 1 \leqslant l \leqslant i,$$

$$1 \leqslant d_l \leqslant N \quad \text{if } i < l \leqslant j. \tag{20}$$

Using again the principle of inclusion and exclusion, we get

$$\tilde{P}_{ji}=\sum_{m=-m_{max}}^{m_{max}}\sum_{l=0}^{j}(-1)^l\sum_{p=0}^{\min(l,j-i)}\binom{j-i}{p} \times\binom{i}{l-p}\cdot\binom{Nf_N(p,l,m)+j-1}{j-1}\Theta(f_N(p,l,m)), \tag{21}$$

where $\Theta(x)$ is the Heaviside (or step) function [$\Theta(x)=1$ for $x>0$ and $\Theta(x)=0$ otherwise] and

$$f_N(p,l,m) = \frac{i}{2} - m + p - l + \gamma\left(\frac{j-i}{2} - p\right) - \frac{p + i/2}{N}. \tag{22}$$

As we are only interested in the dominant terms of $\tilde{P}_{ij}$, we develop it in powers of N to get

$$\tilde{P}_{ji} = N^{j-1} \sum_{m=-m_{max}}^{m_{max}} \sum_{l=0}^{j} (-1)^l \sum_{p=0}^{min(l,j-i)} \binom{j-i}{p}\binom{i}{l-p} \times \left[\frac{f_\infty^{j-1}}{(j-1)!} + N^{-1}\frac{f_\infty^{j-2}}{(j-2)!}\left(\frac{j-i}{2} - p\right) + O(N^{-2})\right]\Theta(f_\infty), \tag{23}$$

where

$$f_\infty = f_\infty(p,l,v) = \frac{i}{2} - m + p - l + \gamma\left(\frac{j-i}{2} - p\right). \tag{24}$$

For the first-order term of Eq. (23), the sums can be performed (see the Appendix) to obtain the simple result

$$\tilde{P}_{ji} \sim N^{j-1}\gamma^{j-i} \quad \text{for } 1 \leqslant i \leqslant j. \tag{25}$$

For $\tilde{P}_{j0}$ there is not such a simple expression. On the other hand, $\tilde{P}_{j0} = P_{j0}$. Thus, $\tilde{P}_{j0}$ is the number of j-cycles of a graph with only short links—that is, a circulant graph. Thus, it can be written as

$$\tilde{P}_{j0} = P_{j0} = \sum_{l=0}^{N-1} \lambda_l^j, \tag{26}$$

where the λ's are the eigenvalues of a circulant matrix, given by Eq. (12).

Using all this, the number of ji-cycles can be calculated, giving

$$P_{ji} = (-1)^i(P_{j0} - N^{j-1}\gamma^j) + N^{j-1}\gamma^{j-i}(1-\gamma)^i. \tag{27}$$

Using this and Eq. (16), we obtain, for the first order of the moments of a dense partially random matrix,

$$M_j = (P_{j0} - \gamma^j N^{j-1})(p_1 - p_2)^j + \gamma_*^j N^{j-1} \quad \text{for } j \geqslant 3, \tag{28}$$

where $\gamma_* = p_1\gamma + p_2(1-\gamma)$ is the average degree of a vertex. The spectrum of eigenvalues that generates the moments corresponding to Eq. (28), *for all values of* j (i.e., not only for $j \geqslant 3$), satisfies $\lambda_1/N \to \gamma_*$ and $\lambda_j/N \to (p_1 - p_2)\lambda_j^c/N$ for $j \geqslant 1$. Notice that this would imply that the whole spectrum is only a rescaling of the spectrum of the substrate (only the first eigenvalue is scaling differently). But the problem is that, because of the symmetry of the matrices, the second moment is, to first order, $M_2 = N\gamma_*$, clearly different to what would be obtained by setting $j=2$ in Eq. (28) (**$M_{j=2} = N[(\gamma - \gamma^2)(p_1 - p_2)^2 + \gamma_*]$**). This means that not all the eigenvalues can tend to the values mentioned above.

On the other hand, the fact that $M_j = O(N^{j-1})$ implies [see Eq. (15)] that every eigenvalue that satisfies $|\lambda| = O(N)$ must tend to $(p_1 - p_2)\lambda^c$. And from Eq. (13) it can be seen that the number of such eigenvalues diverges with N. But the number of eigenvalues that *do not* tend to λ_c, which satisfy $|\lambda| = o(N)$, must also diverge with N; otherwise, its influence would not be felt in M_2.

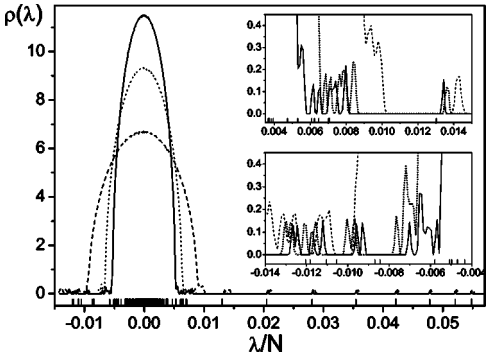

FIG. 3. Average distribution of eigenvalues for $G_{p_1}(\gamma)$ with $\gamma = 0.1$ and $p_1 = 0.6$, for $N = 3001$ (dashed line), $N = 6001$ (dotted line), and $N = 9001$ (solid line). The averages were taken over 100, 30, and 10 matrices, respectively. The small vertical bars over the horizontal axis show the first-order predictions for the discrete part of the spectrum, extended to all values of λ.

In Fig. 3 we show the distribution of eigenvalues for matrices with $N = 6001$. It can be seen that the largest eigenvalues are very close to the values predicted and the deviations are larger for smaller values of λ/N. But for small values of λ the spectrum seems to be continuous and similar to a semicircle distribution.

If we *assume* that the distribution is given by a discrete part, where to dominant order $\lambda_j \sim \lambda_j^c$ and a continuous part given by a semicircle distribution (to dominant order), the second moment can be used to determine the width of the semicircle. It is known [18] that the semicircle distribution

$$\rho_s(\lambda) = \begin{cases} \dfrac{2}{\pi\sigma^2}\sqrt{\sigma^2 - \lambda^2}, & \text{for } -\sigma \leqslant \lambda \leqslant \sigma, \\ 0, & \text{otherwise}, \end{cases} \tag{29}$$

generates moments

$$M_{2j}^s = \int d\lambda \lambda^{2j}\rho_s(\lambda) = \frac{2j!}{j!(j+1)!}(\sigma/2)^{2j} \tag{30}$$

(odd moments vanish because of the symmetry.) From Eq. (28), extended to $j=2$, we know that to obtain the correct value of the second moment for the whole distribution, the continuous part should satisfy $M_2^c = N[\gamma_* - \gamma_*^2 - (\gamma - \gamma^2)(p_1 - p_2)^2]$. For this, the width of the semicircle must be

$$\sigma = 2\sqrt{N[\gamma_* - \gamma_*^2 - (\gamma - \gamma^2)(p_1 - p_2)^2]}. \tag{31}$$

To test the correctness of this assumption, we have used it to scale the average of the continuous part of the spectrum of $G_{p_1}(\gamma)$ for several values of N and p_1. The results, displayed in Fig. 4, show that this scaling collapses all the curves onto the unit semicircle, as predicted. Notice that the deviation from the semicircle is only noticeable for large values of p_1, because in this case the discrete part of the spectrum contains a significant part of the eigenvalues, thus partially depleting and skewing the semicircle.

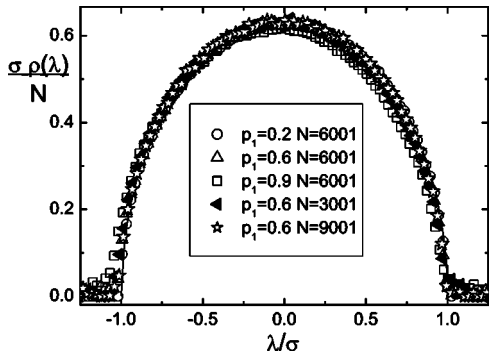

FIG. 4. Scaling of the average of the continuous part of the spectrum for $G_{p_1}(\gamma)$ with $\gamma=0.1$, for different values of p_1 and N. The averages for $N=3001$, $N=6001$, and $N=9001$ have been taken over 100, 30, and 10 matrices, respectively. The solid line shows the theoretical prediction (semicircle distribution).

To confirm analytically the existence of the semicircle, one should develop the moments to an order large enough in the corrections to see the contribution of the semicircle. The problem is that, whereas the order of magnitude of M_j^d is N^{j-1}, the semicircle generates moments $M_j^s=O(N^{j/2})$. Thus, for high values of j the contribution of the semicircle lies deeply buried under the ones of the discrete part of the spectrum. Nevertheless, we have calculated the moments to second order (see next subsection) and confirmed that the semicircle provides the right value for M_4.

The existence of the semicircle imposes a limit on the number of eigenvalues in the discrete part: it must contain only the eigenvalues that satisfy $|\lambda|>\sigma$. Equation (13) implies that the number of such eigenvalues is proportional to $N/\sigma=O(\sqrt{N})$.

Putting all this together the complete eigenvalue distribution of DPRG's is, to first order in N,

$$\rho(\lambda) = \begin{cases} \dfrac{2(N-N_\sigma)}{\pi\sigma^2 N}\sqrt{\sigma^2-\lambda^2}, & -\sigma \leqslant \lambda \leqslant \sigma, \\ \dfrac{2}{N}\sum_{j=0}^{\infty}\delta\left(\lambda - N(p_1-p_2)\dfrac{\sin(\pi j\gamma)}{\pi j}\right), & \text{otherwise}, \end{cases} \tag{32}$$

where N_σ is the number of values of j such that $N(p_1-p_2)\times[\sin(\pi j\gamma)/\pi j]>\sigma$—i.e., the number of eigenvalues contained in the discrete part. It must be remarked that even though these eigenvalues are degenerated, this degeneracy breaks down for finite values of N. Nevertheless, in our simulations their separation is so small as to make them statistically indistinguishable inside each peak, for the values of N chosen.

Second-order calculation

To go beyond the dominant order in the calculation of the moments, two different contributions must be taken into account.

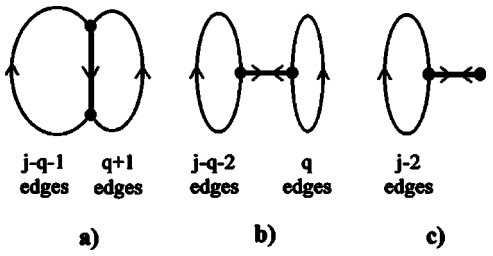

FIG. 5. Schematic representation of the possible cycles with only one repeated edge. The legends indicate the number of edges present in each subcycle. The edge traversed twice is shown as a thick line.

The first contribution is simply a refinement of the calculation of $\tilde{P}_{ji}$ for $i>0$,[1] which can be split in two terms. One of them is simply what one gets when using the second-order term from the development of $\tilde{P}_{ji}$ [see Eq. (23)]. This gives $\tilde{P}_{ji}^{(2)}=i\tilde{P}_{j-1\ i-1}$. The other part arises when we subtract from Eq. (21) the paths with loops—i.e, the solutions of Eq. (19) having $d_l=0$ for some values of l (which were introduced to make calculations easier). The number of such solutions is $O(N^{j-l-1})$. Thus, for the second-order calculation we need to subtract from Eq. (21) the number of solutions with only one vanishing distance, which is $iP_{j-1\ i-1}+(j-i)P_{j-1\ i}$. Adding these two terms and using Eqs. (18) and (16), the first contribution to the correction of the moments is obtained:

$$\Delta M_j^I = \Delta P_{j0}(p_1-p_2)^j - p_2 j M_{j-1}, \tag{33}$$

where ΔP_{j0} is the first correction to P_{j0}.

The second contribution originates in the fact that the weight assigned to each cycle in Eq. (16), $p_1^{j-i}p_2^i$, implies that all the edges traversed in each cycle are different. To correct this, some paths have to be reweighted. But the number of j-cycles with r edges repeated is $O(N^{j-1-r})$ or smaller; thus, we only need to consider cycles with one edge repeated. But there are only two possible classes of such cycles, as shown in Fig. 5: the first class consists of two cycles sharing an edge which is traversed in only one direction, and the second class consists of two cycles joined by an edge which is traversed in both directions. For the first class [Fig. 5(a)], the number of cycles is $O(N^{j-q-2})O(N^{q-1})=O(N^{j-3})$ for all possible values of q. Notice that in this case q must be positive for the edge to be traversed twice. The number of possible j-cycles for the second class [Fig. 5(b)] is proportional to $O(N^{j-q-3})\times N\times O(N^{q-1})=O(N^{q-3})$ if $q\geqslant 2$ and $O(N^{j-3})N=O(N^{j-2})$ if $q=0$. Therefore, the contribution of dominant order, given by those paths with $q=0$ [shown in Fig. 5(c)], can be written

$$\Delta M_j^{II} = \Delta\gamma j N M_{j-2} \quad \text{for } j\geqslant 5, \tag{34}$$

where $\Delta\gamma=\gamma(p_1-p_1^2)+(1-\gamma)(p_2-p_2^2)$. jN is the number of possibilities for the choice of the edge that will be repeated,

[1]Although the correction for $\tilde{P}_{j0}$ can in principle be calculated, we do not care about the specific functional form of it, because the correction to the eigenvalues that give rise to this term can be directly obtained from Eq. (13).

the two terms in $\Delta\gamma$ correspond to the possibility that the repeated term is a short or a long link, and M_{j-2} is the number of cycles of length $j-2$.

Notice that to obtain Eq. (34) we have only corrected the weight of the repeated edge, assuming that in the closed part of the paths considered (corresponding to the ovals in Fig. 5) all edges are different. For $j>4$ this is correct, because the number of such subcycles needing reweighing is of second order with respect to the total. But this is not so for $j=4$. In this case, the oval in Fig. 5(c) corresponds to a single edge traversed twice. Taking this into account, the right contribution to the correction of M_4 is

$$\Delta M_4^{II} = 4N^2(\gamma_*^2 - \gamma_{**}), \tag{35}$$

where $\gamma_{**}=p_1^2\gamma+p_2^2(1-\gamma)$.

Adding both contributions, the first correction to M_j can be written as

$$\Delta M_4 = (p_1-p_2)^3[\Delta P_{40}(p_1-p_2) - 4p_2(P_{30}-N^2\gamma^3)] + N^2[2(\gamma_*^2-\gamma_{**}^2) - 4p_2\gamma_*^3], \tag{36}$$

$$\Delta M_j = j(p_1-p_2)^{j-2}(P_{j-20}-N^{j-1}\gamma^{j-2})\Delta\gamma - (p_1-p_2)^{j-1}jp_2(P_{j-10}-N^{j-2}\gamma^{j-1}) + jN^{j-2}(-p_2\gamma_*^{j-1}+\gamma_*^{j-2}\Delta\gamma) + (p_1-p_2)^j\Delta P_{j0} \quad \text{for } j\geqslant 5. \tag{37}$$

Consider now the distribution of eigenvalues that has been proposed to generate these moments. We must introduce corrections to it, to account for the calculated corrections to the generated moments. For $j\geqslant 4$ only the corrections to the discrete part of the distribution are needed. In terms of the first-order term of the development of the eigenvalues, the correction to the jth moment is

$$\Delta M_j = j\sum_{i=0}^{N}\lambda_i^{j-1}\Delta\lambda_i. \tag{38}$$

Replacing this on the left-hand side of Eq. (37) and using that the same holds for the corrections to the moments of the substrate ($\Delta P_{j0}=\Delta M_j^d$), a comparison of terms in both sides of the resulting equation gives

$$\Delta\lambda_i = \Delta\lambda_i^0 - p_2 + \lambda_i^{-1}\Delta\gamma. \tag{39}$$

But by construction, these corrections to the discrete eigenvalues generate the right corrections only to the moments of order larger than the fourth. For the fourth moment this discrepancy must be bridged by the corresponding moment generated by the continuous part of the spectrum. But

$$\Delta M_{j=4} - \Delta M_4 = 2(\gamma_* - \gamma_{*2})^2, \tag{40}$$

which is exactly the fourth moment generated by the semicircle distribution given in Eq. (29).

C. Higher-dimensional substrates

The results obtained in the preceding sections can be extended to DPRG's defined on higher-dimensional substrates. These substrates are defined as hypercubic lattices in d dimensions where each node is connected to a hypercube of $k_1k_2\cdots k_d$ other nodes. As already mentioned, we assume that the hypercube is closed, in the sense that nodes at the boundaries of the hypercube are considered nearest neighbors of the nodes at the opposite boundary.

In a d-dimensional DPRG a ji-cycle can be represented as a succession of j distances $\vec{d}_l\in\mathbb{Z}^d$. Componentwise, this can be regarded as the superposition of d unidimensional subcycles. Notice that the number of shortcuts used in each subcycle is *smaller than or equal to* i. To build a d-dimensional ji-cycle out of unidimensional paths, only the following condition must be satisfied. Let us call $\{i\}$ the set of steps of the d-dimensional ji-cycle that traverse shortcuts and $\{i_l\}$ its analog for the subcycle in the lth dimension ($1\leqslant l\leqslant d$). The condition is then that the *union* of all the sets $\{i_l\}$ be equal to $\{i\}$: $\cup_{l=1}^d\{i_l\}=\{i\}$.

Therefore, counting the number of possible ji-cycles is equivalent to counting the number of unidimensional subcycles satisfying this condition. This can be written as

$$P_{ji}(d) = \prod_{l=1}^{d}\sum_{i_l=0}^{i-s_l}\binom{i-s_l}{i_l}\left[\prod_{q=1}^{l-1}\binom{i_q}{i_{ql}}\right]P_{ji_l+s_{ll}}^l, \tag{41}$$

with $s_l=\Sigma_{q=1}^{l-1}i_q$ and $s_{ll}=\Sigma_{q=1}^{l-1}i_{ql}$. P_{ji}^l is the number of ji-paths in the lth dimension. Notice that i_{lq} is the size of the intersection of sets $\{i_l\}$ and $\{i_q\}$. The evaluation of this expression is cumbersome but straightforward, giving

$$P_{ji}(d) = (-1)^i[P_{j0}(d) - N^{j-1}\gamma_d^j] + N^{j-1}\gamma_d^{j-i}(1-\gamma_d)^i, \tag{42}$$

where $P_{j0}(d)=\Pi_{l=1}^d P_{j0}^l$, and $\gamma_d=\Pi_{l=1}^d\gamma(l)$.

Using this and Eq. (16), we obtain, for the first order of the moments,

$$M_j = [P_{j0}(d) - \gamma_d^jN^{j-1}](p_1-p_2)^j + [p_1\gamma_d + p_2(1-\gamma_d)]^jN^{j-1} \tag{43}$$

for $j\geqslant 3$. Using the same reasoning of Sec. IV B we see that the eigenvalues satisfying $|\lambda|=O(N)$ must tend to those of the substrate, rescaled by the disorder: $\lambda_{j_1j_2\cdots j_d}\sim(p_1-p_2)\lambda^c_{j_1j_2\cdots j_d}$, where $\lambda^c_{j_1j_2\cdots j_d}$ are given by Eq. (14).

In analogy to the one-dimensional case, for the smaller eigenvalues we can conjecture the presence of a continuous distribution following a semicircle law, because of the discrepancy between the real second moment and the one generated by the discrete distribution. Unfortunately, this conjecture cannot be tested for all values of d in the same way used for the unidimensional case in Sec. IV B. The reason for this is that, as the moments are obtained as sums of products of d unidimensional moments, their development involves powers of $N^{1/d}$. But the moments generated by the semicircle are $O(N^{j/2})$. Thus, for M_4 its contribution must be searched in the dth correction to the real fourth moment, whose evaluation, even though straightforward in principle, gets extremely cumbersome even for small values of d.

Fortunately, for most applications one only needs the largest eigenvalues in absolute value (see Sec. V for some examples), which are given by the discrete part of the distribution. And if a function of all the eigenvalues is needed, it can always be rewritten as a series involving the moments.

D. Comparisons

The limit of small γ should give us an idea of the approximate form of the spectrum for sparse SWG's. In this limit, Eqs. (4) and (5) give $p_1 \simeq 1-p$ and $p_2 \simeq \gamma p$. From Eq. (32), one can see that, at least for not too large values of j, $\lambda_j \sim p_1 \lambda_0^c$, for small γ. Thus, the eigenvalues accumulate at a distance of $p\gamma N$ from the Frobenius-Perron eigenvalue $\lambda_0 = \gamma N$, with a trail of eigenvalues reaching to the edges of the semicircle. In the small-γ limit, the width of the semicircle is $\sigma \simeq 2\sqrt{2N\gamma(2p-p^2)}$.

For small values of p the eigenvalues accumulate so close to the Perron-Frobenius eigenvalues that the gap should only be visible for very large values of N. The continuous part of the distribution, whose width is proportional to $\sqrt{p}$, gets very small and contains few eigenvalues, so its shape becomes very irregular and skewed to the negative side (to retain the vanishing of the first moment). This picture is very similar to what can be seen in Fig. 3(b) of Ref. [4].

If p is not small, the accumulation point is clearly separated from the Frobenius-Perron eigenvalue. Besides, σ can be close to $\sqrt{N\gamma}$, thus including enough eigenvalues to take a shape close to the semicircle. This shape should also be skewed. This picture is very similar to what can be seen in Fig. 3(c) of Ref. [4].

It is also similar to what was found in Ref. [22]. In the graphs considered in that article links are *added* to a sparse substrate (i.e., they are not *rewired*). The dense version of this corresponds to taking $p_1 = 1$ in our model. Even though it is the spectrum of the Laplacian matrix that is studied, the results can be translated very easily to the spectrum of the adjacency matrix, because for large sizes the graphs can be considered regular, in which case the eigenvalues of both matrices can be related by the formula $\lambda^L = k - \lambda^A$. It is found that two peaks appear. The closest to the Perron-Frobenius eigenvalue is separated from it by a pseudogap (i.e., an interval where there are eigenvalues, but very few of them). This peak is found to be "in quantitative agreement with the ring spectrum" and can be related to the accumulation point mentioned above. The other peak, which is very irregular for a small number of shortcuts, can be related to the continuous part of the spectrum found in DPRG's.

V. SOME APPLICATIONS

It is interesting to notice that the average distance and the clustering coefficient present qualitatively the same behavior as that seen in sparse SWG's. We can see that for small values of p_1 the graphs obtained have average distances which are close to those in random graphs, while retaining a clustering coefficient close to the values present in circulant graphs. Naturally the range of values spanned by (the logarithm of) both quantities is much larger in SWG's.

Having the distribution of eigenvalues or, equivalently, the expression for all the moments allows one to calculate or at least to bound many processes that can take place in DPRG's.

For regular graphs (i.e., graphs where all vertices have the same degree), the spectrum of the adjacency matrix can be very simply related to the spectrum of the *Laplacian* matrix, defined by $L = D - A$ where A is the adjacency matrix and D is the degree matrix (a diagonal matrix such that d_{ii} is the degree of vertex i) and the *normal* matrix $N = D^{-1}A$. The Laplacian has very interesting properties and many applications in physics, especially because it arises in the discretization of the Laplacian operator [23]. As SWG's are regular, their Laplacian and adjacency matrix eigenvalues are related by $\lambda^L = k - \lambda^A$. If the eigenvalues are ordered from small to large, the first eigenvalue is $\lambda_0^L = 0$. The second eigenvalue is probably the most important as it can be related to a number of properties of processes taking place in such graphs.

In the following we show a couple of examples where we apply the results obtained in the preceding sections.

A. Mixing rate

A random walk on a graph is defined as a Markov chain where the probability of jumping from vertex i to vertex j is $1/d_i$ if they are connected and 0 otherwise [16]. Several properties of random walks can be related to the spectrum of a graph. For every time t there will be a different probability $P_t(j)$ of finding the walker on a site j. A stationary distribution is defined by the requirement that $P_t = P_{t+1}$ for $t > T$, for some T. $\pi(j) = d_j/2M$ is a stationary distribution, and for regular graphs it is unique. It can be shown that, regardless of their initial state, all the walks tend to this distribution, provided the graph is connected and not bipartite.

When the walk has reached the stationary distribution it has essentially lost all memory of its initial state (or distribution) and all the vertices are sampled with probability proportional to their connectivity, which is useful for several algorithms. But how fast is the convergence to the stationary distribution? One of the possible measures of this is the *mixing rate*, defined as

$$\mu = \limsup_{t\to\infty} \max_{i,j} |p_{ij} - d_j/M|^{1/t}. \tag{44}$$

It can be shown [16] that $\mu = \lambda_L^N$, the largest nontrivial eigenvalue of the normal matrix. Using Eqs. (32) and (4) we obtain

$$\begin{aligned} \mu = \lambda_L^N &= (p_1 - p_2)\frac{\sin(\pi\gamma)}{\pi\gamma} \\ &= \left[\gamma - 1 + \exp\left(-\frac{\gamma p}{1-\gamma}\right)\right]\frac{\sin(\pi\gamma)}{\pi\gamma^2}, \end{aligned} \tag{45}$$

where the last equality is valid for a dense SWG. This shows that for fixed and small γ the mixing rate decreases almost linearly with the disorder. Notice that the fact that the average distance jumps to its minimal value at $p = 0^+$ does not influence the mixing rate.

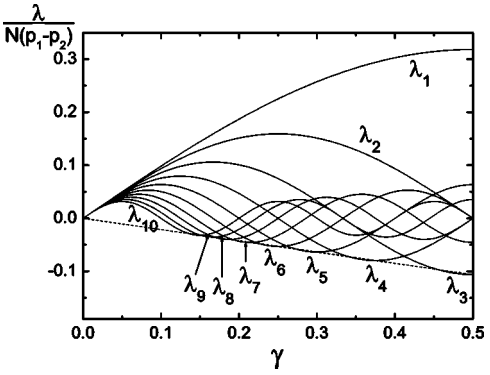

FIG. 6. First ten eigenvalues of the discrete spectrum of the adjacency matrix of a DPRG. The dashed line $[\lambda=-2\gamma N(p_1-p_2)/3\pi]$, which joins the first minima of all the eigenvalues, is a reasonably accurate estimation of the smallest eigenvalue for every γ.

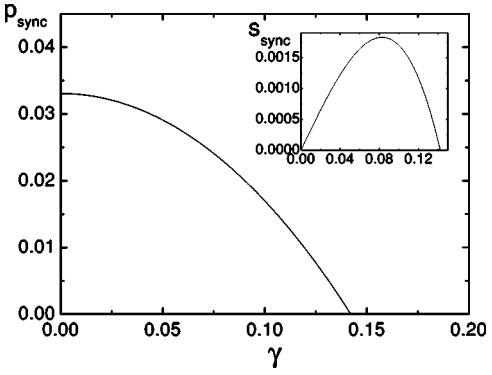

FIG. 7. Synchronization threshold for graphs $G_{p_1}(\gamma)$. The inset shows the critical fraction of links that must be shortcuts.

B. Synchronization of coupled oscillators

One of the most interesting processes that can take place on a network is the collective dynamics of an array of coupled oscillators. And perhaps the most striking collective state is that where all the identical oscillators get *synchronized*. Naturally, synchronization is not always possible; it depends on the specific properties of the oscillators as well as on the topology of the network. In Ref. [24] a very useful formalism was introduced to study the conditions for the existence of a stable synchronized phase for a wide class of oscillators and couplings. The equations of motion for the *i*th oscillator in the network are

$$\mathbf{x}_i = \mathbf{F}(\mathbf{x}_i) + \sigma \sum_{j=1}^{N} L_{ij}\mathbf{H}(\mathbf{x}_j), \tag{46}$$

where **F** governs the dynamics of each individual oscillator, **H** is an arbitrary output function, σ gives the strength of the coupling, and L is the Laplacian matrix of the network. It can be shown [24] that for a system of this form, the condition for the existence of a stable synchronous state reduces to

$$\lambda_L^L/\lambda_S^L < \beta, \tag{47}$$

where λ_L^L and λ_S^L are, respectively, the largest and smallest nontrivial eigenvalues of the Laplacian. β is a parameter that depends only on the oscillators and its coupling, and not on the topology. $\beta \in [5,100]$ for several chaotic oscillators [25].

Using Eq. (47) we can calculate the synchronizability threshold for dense SWG's. For DPRG's and sufficiently large values of N the smallest and largest (excluding the Frobenius-Perron) eigenvalues of the adjacency matrix are located in the discrete part of the spectrum. The largest nontrivial eigenvalue is always $\lambda_L^A = N[(p_1-p_2)\sin(\pi\gamma)]/\pi$, but the index of the smallest eigenvalue depends on γ (see Fig. 6) An approximation to it is given by $\lambda_S^A = -N\gamma(p_1-p_2)2/3\pi$, which is accurate enough for our illustrative purposes.

The synchronizability threshold is defined as the smallest value of p for which the system becomes synchronizable. Using the already mentioned relation between the adjacency and Laplacian matrices, the synchronization condition for DPRG's becomes

$$\frac{\beta-1}{p_1-p_2} < \frac{2}{3\pi} + \frac{\beta\sin(\gamma\pi)}{\gamma\pi}. \tag{48}$$

Notice that dense random graphs are always synchronizable, as $\lambda_L/\lambda_S=1$. As was done in Ref. [25] we have calculated the synchronization threshold for a dense SWG for the case of a system of oscillators with $\beta=37.85$. The results are displayed in Fig. 7.

The region below the curves gives the set of parameters for which the system is *not* synchronizable. It is interesting to notice that this implies that to obtain a synchronizable system it is not enough to have a macroscopic number of shortcuts. Also, the fact that in this region p is positive shows that the onset of synchronization does not depend on the average distance because, as we have seen in Sec. III A, for $p>0$ the average distance is the smallest possible. This supports the idea that average distance alone is not a relevant factor for the onset of synchronization. But in Ref. [26] it has been argued that synchronization seems to depend on the combined effects of small average distance and uniformity of the connectivity distribution. Yet our results show that it must at least depend on some additional factors. For fixed values of γ we have seen that the synchronization threshold is $p_t>0$, even though all graphs $G_p(\gamma)$ have the same connectivity ($N\gamma$ connections per node) and the same average distance for $p>0$.

VI. CONCLUSIONS

In this article we have studied some properties of dense partially random graphs that can be obtained by adding edges with probability p_2 to a dense ordered substrate and then deleting the original edges of the substate with probability $1-p_1$. We have found that they show qualitatively the same behavior as the corresponding properties of sparse graphs, in particular small-world graphs. For the average distance we find that, for any macroscopic number of shortcuts, it falls to its minimum possible value (in the infinite-size limit). We show that the clustering coefficient decays slowly, thus al-

lowing for a range of parameters where the graphs have relatively large clustering and minimal average distance.

By counting cycles on the graph, we have obtained the distribution of eigenvalues of the adjacency matrix. We found that it consists of two parts: a discrete one where the eigenvalues, of order N, are simply rescalings of the corresponding eigenvalues of the substrate and a continuous part given by a semicircle distribution whose width is of order $\sqrt{N}$ and is proportional to the disorder. It is interesting to notice that a similar form of the spectrum has been obtained [27] for matrices that are the sum of a stochastic matrix and a block matrix. The block matrix is composed of k blocks of size proportional to N where all off-diagonal components are equal. The spectrum obtained consists of a semicircle distribution of width proportional to $\sqrt{N}$ and a discrete part containing the k largest eigenvalues (of order N). Notice that in our case the discrete part contains a diverging number of eigenvalues.

We have shown how the distribution found can be useful to understand the distributions that arise in the numerical study of the spectrum of sparse small-world graphs. In the studies published so far two peaks appear and a pseudogap separates the bulk of the spectrum from the Frobenius Perron eigenvalue. Comparing with our results for small values of the connectivity, one of the peaks can in principle be associated with large eigenvalues of the substrate, all rescaled by the same value (dependent on the disorder), and the other to a continuous distribution of small width that is usually a signature of disorder.

We have applied our results to the calculation of the mixing rate of a random walk on the graph and to the calculation of the synchronization threshold of a system of coupled oscillators placed on the nodes of the graph. We have shown that below and above the threshold there exist graphs with the same average distance and the same connectivity (i.e., the same number of connections per vertex). Previously it has been argued that a combination of these two factors was responsible for the onset of synchronizability. Our results show that there must at least exist more quantities involved.

ACKNOWLEDGMENT

I acknowledge support from the Centro Latinoamericano de Física.

APPENDIX

Here we sketch the calculation that leads to Eq. (25). Although we suspect that there must be a shorter path to Eq. (25), we have not been able to find it.

We begin by splitting the dominant term in Eq. (23), $\tilde{P}^{(1)}_{ji}$, into two parts:

$$\tilde{P}^{(1)}_{ji} = \sum_{m=-m_{\max}}^{m_{\max}} \sum_{l=0}^{j} (-1)^l \sum_{p=0}^{\min(l,j-i)} \binom{j-i}{p}\binom{i}{l-p} \frac{N^{j-1}}{(j-1)!} \times g\left[i/2 - m + p - l + \gamma\left(\frac{j-i}{2} - p\right)\right] = \frac{N^{j-1}}{(j-1)!}(\mathbf{A}+\mathbf{B}), \tag{A1}$$

where $g(x)=x^{j-1}\theta(x)$ and

$$\mathbf{A} = \sum_{m=-m_{\max}}^{m_{\max}} \sum_{l=j-i}^{j} (-1)^l \sum_{p=0}^{j-i} \binom{j-i}{p}\binom{i}{l-p} \times g\left[i/2 - m + p - l + \gamma\left(\frac{j-i}{2} - p\right)\right] \tag{A2}$$

$$\mathbf{B} = \sum_{m=-m_{\max}}^{m_{\max}} \sum_{l=0}^{j-i-1} (-1)^l \sum_{p=0}^{l} \binom{j-i}{p}\binom{i}{l-p} \times g\left[i/2 - m + p - l + \gamma\left(\frac{j-i}{2} - p\right)\right]. \tag{A3}$$

Notice that, to avoid overloading the notation, we extend the definition of the combinatorial numbers,

$$\binom{a}{b} = \frac{a!}{(a-b)!\,b!}$$

for $b \leqslant a$, to

$$\binom{a}{b} = 0$$

for $b > a$. By making the replacements $p \to j-i-p$ and $l \to j-i-l$, and rearranging the sums, we obtain

$$\mathbf{A} = \sum_{m=-m_{\max}}^{m_{\max}} \sum_{p}^{j-i} {}' \sum_{l=0}^{i-p} (-1)^{l+j-i}\binom{i}{l+p}(-1)^l \times g(i - v - p - l + \gamma p) = \mathbf{A}' - \mathbf{B}', \tag{A4}$$

where $\Sigma_i^{a\prime} = \Sigma_{i=0}^{a}(-1)^{i\binom{a}{i}}$ is an operator and

$$\mathbf{A}' = (-1)^j \sum_{p}^{j-i} {}' \sum_{l}^{i} {}' \sum_{m=0}^{2m_{\max}} g(v + l + \gamma p - \alpha), \tag{A5}$$

$$\mathbf{B}' = (-1)^{j-i} \sum_{m=0}^{2m_{\max}} \sum_{p=1}^{j-i} (-1)^p \binom{j-i}{p} \sum_{l=0}^{p-1} (-1)^l \binom{i}{l} \times g(v + l + \gamma p - \alpha). \tag{A6}$$

By manipulating the indices and reordering the sums, it is not difficult to show that $\mathbf{B}=\mathbf{B}'$. Using the definition of α, we can show that $[l+\gamma p-\alpha] < 2m_{\max}$. Thus

$$\begin{aligned}\mathbf{A}' &= (-1)^j \sum_{p}^{j-i} {}' \sum_{l}^{i} {}' \sum_{m=-l}^{[\gamma p-\alpha]} (-m + \gamma p - \alpha)^{j-1} \\ &= \sum_{p}^{j-i} {}' \sum_{l=1}^{i} (-1)^{l-i}\binom{i}{l} \sum_{m=-l}^{1} (-m + \gamma p - \alpha)^{j-1} \\ &\quad + \sum_{p=[\alpha/\gamma]}^{j-i} (-1)^{p-j}\binom{j-i}{p} \sum_{l}^{i} {}' \sum_{m=0}^{[\gamma p-\alpha]} (-m + \gamma p - \alpha)^{j-1}.\end{aligned} \tag{A7}$$

It is known [21] that

$$\sum_{k}^{a}{}' k^n = \begin{cases} (-1)^a a!\, S(n,a) & \text{for } 0 < a \leqslant n, \\ 0 & \text{for } a > n, \end{cases} \tag{A8}$$

where $S(n,a)$ are the Stirling numbers of the second kind [21]. Using Eq. (A8) one sees that the term in the last line of Eq. (A7) vanishes (but notice that this can only happen for $i>0$). Thus, expanding in powers of m, we get

$$\mathbf{A}' = \sum_{p}^{j-i}{}' \sum_{l=1}^{i} (-1)^{l-j} \binom{i}{l} \sum_{k=0}^{j-1} (\gamma p - \alpha)^{j-1-k} \sum_{m=1}^{l} m^k. \tag{A9}$$

Bernoulli's expression for a sum of powers [28] is $\Sigma_{m=1}^{l} m^k = \Sigma_{v=1}^{k+1} b_{km} l^v$ where

$$b_{km} = \frac{(-1)^{k-m+1}}{k+1} \binom{p+1}{k} B_{k-m+1}$$

and B_i are the Bernoulli numbers. Using this and summing over l, we get

$$\mathbf{A}' = \sum_{k=i-1}^{j-1} \binom{j-1}{k} \sum_{v=i}^{k+1} b_{vk} (-1)^{v-j} i!\, S(v,i) \sum_{p}^{j-i}{}' (\gamma p - \alpha)^{j-1-k}. \tag{A10}$$

But Eq. (A8) shows that in Eq. (A9) the sum over p vanishes for $k>i-1$. Thus, only one term survives, the one with $k=i-1$. Using that $B_0=1$ and $S(i,i)=i!$ we finally obtain

$$\tilde{P}_{ji} \sim \frac{N^{j-1}}{(j-1)!} \mathbf{A}' = N^{j-1} \gamma^{j-i}. \tag{A11}$$

[1] F. Y. Wu, J. Stat. Phys. **52**, 99 (1988).
[2] P. Erdös and A. Renyi, Publ. Math. (Debrecen) **6**, 290 (1959).
[3] D. J. Watts and S. Strogatz, Nature (London) **393**, 440 (1998).
[4] I. J. Farkas, I. Derényi, A.-L. Barabási, and T. Vicsek, Phys. Rev. E **64**, 026704 (2001).
[5] P. Sen, S. Dasgupta, A. Chatterjee, P. A. Sreeram, G. Mukherjee, and S. S. Manna, Phys. Rev. E **67**, 036106 (2003).
[6] A. Wagner and D. A. Fell, Proc. R. Soc. London, Ser. B **268**, 1803 (2001).
[7] S. Light and P. Kraulis, BMC Bioinformatics **5**, 15 (2004).
[8] A. P. S. de Moura, Y.-C. Lai, and A. E. Motter, Phys. Rev. E **68**, 017102 (2003).
[9] D. J. Watts, *Small Worlds: The Dynamics of Networks between Order and Randomness* (Princeton University, Princeton, NJ, 1999).
[10] B. Bollobás, *Random Graphs* (Cambridge University Press, Cambridge, England, 2001).
[11] W. S. Lovejoy and C. H. Loch, Soc. Networks **25**, 333 (2003).
[12] M. E. J. Newman, S. H. Strogatz, and D. J. Watts, Phys. Rev. E **64**, 026118 (2001).
[13] A. Barrat and M. Weigt, Eur. Phys. J. B **13**, 547 (1999).
[14] N. Biggs, *Algebraic Graph Theory* (Cambridge University Press, Cambridge, England, 1974).
[15] F. R. K. Chung, *Spectral Graph Theory* (American Mathematical Society, Providence, RI, 1997).
[16] L. Lovász and P. Winkler, in *Microsurveys in Discrete Probability*, edited by D. Aldous and J. Propp, DIMACS Series in Discrete Mathematics and Theoretical Computational Science (AMS, Providence, RI, 1998), pp. 85–133.
[17] R. M. Gray (unpublished). Recently updated electronic version available at www-ee.stanford.edu/gray/toeplitz.html
[18] E. P. Wigner, Ann. Math. **62**, 548 (1955).
[19] L. Arnold, J. Math. Anal. Appl. **20**, 262 (1967).
[20] M. Bauer and O. Golinelli, J. Stat. Phys. **103**, 301 (2001).
[21] J. H. van Lint and R. M. Wilson, *A Course in Combinatorics* (Cambridge University Press, Cambridge, England, 1992).
[22] R. Monasson, Eur. Phys. J. B **12**, 555 (1999).
[23] B. Mohar, *Graph Theory, Combinatorics and Applications* (Wiley, New York, 1991), Vol. 2, pp. 871–898.
[24] L. M. Pecora and T. L. Carroll, Phys. Rev. Lett. **80**, 2109 (1998).
[25] M. Barahona and L. M. Pecora, Phys. Rev. Lett. **89**, 054101 (2002).
[26] T. Nishikawa, A. E. Motter, Y.-C. Lai, and F. C. Hoppensteadt, Phys. Rev. Lett. **91**, 014101 (2003).
[27] M. Bolla, Linear Algebr. Appl. **377**, 219 (2004).
[28] K. Ireland and M. Rosen, *A Classical Introduction to Modern Number Theory* (Springer-Verlag, New York, 1998).